Acta Cryst. (1998). B54, 211–220

Monoclinic and Hexagonal Nepheline Structures of $(Na_{3/4}K_{1/4})AlGeO_4$

ROBERT P. HAMMOND AND JACQUES BARBIER*

Department of Chemistry, McMaster University, 1280 Main Street West, Hamilton, Ontario, Canada L8S 4M1. E-mail: barbier@mcmaster.ca

(*Received 24 March 1997; accepted 6 October 1997*)

Abstract

Hexagonal $(Na_{3/4}K_{1/4})AlGeO_4$ crystallizes in the space group $P6_3$ with unit-cell parameters a = 10.164 (2), c = 8.540 (2) Å and Z = 8 [$wR(F^2)$ = 0.066 for all 3060 independent reflections]. Monoclinic $(Na_{3/4}K_{1/4})AlGeO_4$ crystallizes in the space group $P2_1$ with unit-cell parameters a = 10.0477 (4), b = 8.5764 (4), c = 10.2118 (4) Å, β = 119.035 (1)° and Z = 8 [$wR(F^2)$ = 0.120 for all 3194 independent reflections measured on a twinned crystal]. Both structures belong to the large family of stuffed tridymites, with the Al and Ge atoms occupying tetrahedral sites, and the alkali atoms occupying the cavities of the tetrahedral framework. Hexagonal $(Na_{3/4}K_{1/4})AlGeO_4$ is isostructural with the silicate mineral nepheline $(Na_{3/4}K_{1/4})AlSiO_4$, while monoclinic $(Na_{3/4}K_{1/4})AlGeO_4$ corresponds to a minor distortion of the nepheline structure. Chemical analysis by electron microprobe and structure determination of flux-grown single crystals indicate that the hexagonal form with the chemical formula $(Na_{0.78}K_{0.19})Al_{0.97}Ge_{1.03}O_4$ may be stabilized by an alkali deficiency similar to that found in hexagonal natural nephelines. In contrast, all alkali sites are fully occupied in the monoclinic form of composition $(Na_{0.75}K_{0.25})AlGeO_4$ and the lower symmetry eliminates the oxygen disorder present in the hexagonal form.

1. Introduction

During their investigation into the phase relations in the $(NaK)AlGeO_4$ system, Barbier & Fleet (1988) studied polycrystalline samples of the composition $(Na_{3/4}K_{1/4})AlGeO_4$. Below approximately 1073 K this composition adopts a beryllonite structure, but above this temperature it undergoes a phase transition to a nepheline-like monoclinic unit cell [a = 10.289 (2), b = 10.056 (2), c = 8.579 (2) Å, γ = 119.73 (2)°] until melting between 1373 and 1473 K. The authors also reported that examination of the nepheline-like phase by TEM (transmission electron microscopy) revealed that most of the microscopic crystals were twinned. They proposed that this twinning either occurred during growth as a consequence of the pseudo-hexagonal unit cell or was the result of a hexagonal → monoclinic transformation which occurred during quenching. Although the authors did not observe any evidence for a hexagonal phase, Strunz & Ritter (1961) had previously reported the preparation of a hexagonal $(Na_{3/4}K_{1/4})AlGeO_4$ phase (a = 10.26, c = 8.63 Å) by slowly cooling the melt from 1473 to 1273 K. The structures of both the monoclinic and hexagonal forms of $(Na_{3/4}K_{1/4})AlGeO_4$ have been determined by single crystal X-ray diffraction and are described in the present paper. They are also compared with the structure of natural nepheline, $(Na_{3/4}K_{1/4})AlSiO_4$ (Hahn & Buerger, 1955; Dollase, 1970; Foreman & Peacor, 1970; Simmons & Peacor, 1972).

2. Experimental

Powder samples of $(Na_{3/4}K_{1/4})AlGeO_4$ were prepared using Na_2CO_3 (BDH, reagent grade), K_2CO_3 (BDH, reagent grade), Al_2O_3 (Cerac Chemical Co., 99.2%) and GeO_2 (Cerac Chemical Co., 99.999%). Samples of 0.4 g were prepared from pelleted stoichiometric mixtures of the starting materials. The precursors were heated to 773 K at a rate of 1 K min^{-1} and held there for 16 h to decompose the carbonates. The samples were then fired for 3 d at 1273 K with daily regrinding and pelleting. Powder X-ray diffraction patterns of the products, which confirmed that the samples were single phase, were obtained with a Guinier–Hägg camera and indexed using an alternate setting ($\beta \neq 90°$) of the monoclinic unit cell observed by Barbier & Fleet (1988). No trace of a hexagonal $(Na_{3/4}K_{1/4})AlGeO_4$ phase was observed in these experiments and DTA experiments failed to detect any evidence of a phase transition in monoclinic $(Na_{3/4}K_{1/4})AlGeO_4$.

Twinned crystals of monoclinic $(Na_{3/4}K_{1/4})AlGeO_4$ were grown by the flux method, using a mixture of 38.8 mol% Na_2CO_3, 12.9 mol% K_2CO_3, 42.3 mol% MoO_3 and 6.0 mol% V_2O_5 as a flux. The flux was pre-reacted to decompose the carbonates and then the single-phase $(Na_{3/4}K_{1/4})AlGeO_4$ powder was added as a nutrient, using the ratio 14 g flux and 2 g nutrient. The sample was soaked for 5 d at a temperature of 1223 K and then cooled at a rate of 0.6 K h^{-1} to 1173 K.

When the composition of the flux was altered to 35.5 mol% Na_2CO_3, 11.8 mol% K_2CO_3, 47.4 mol%

Table 1. *Results (given as wt% oxides) of the electron microprobe analysis of α- and β-$(Na_{3/4}K_{1/4})[AlGeO_4]$ flux-grown single crystals*

Oxide	Calculated wt%	α-$(Na_{3/4}K_{1/4})[AlGeO_4]$		β-$(Na_{3/4}K_{1/4})[AlGeO_4]$	
		Analysis 1	Analysis 2	Analysis 1	Analysis 2
Na_2O	12.19	12.46	12.13	12.78	12.71
K_2O	6.18	6.25	6.16	4.44	4.52
Al_2O_3	26.75	26.70	26.60	26.37	26.25
GeO_2	54.88	54.61	54.63	56.96	56.78
Total	100.00	100.02	99.52	100.55	100.26
Formula		$(Na_{0.75}K_{0.25})[Al_{1.00}Ge_{1.00}O_4]$†		$(Na_{0.78}K_{0.19})[Al_{0.97}Ge_{1.03}O_4]$	

† The crystal of the α-phase was used as a calibration standard and its composition was taken as ideal.

MoO_3 and 5.3 mol% V_2O_5 (*i.e.* enriched in MoO_3 and deficient in alkali relative to the original flux), but with the same Na:K ratio of 3:1, the product of the crystal growth experiments was a hexagonal nepheline phase. Single crystals, suitable for X-ray structure determination, were obtained from a sample of 15 g of flux and 1 g of monoclinic $[Na_{3/4}K_{1/4}](AlGeO_4)$, which was soaked for 14 d at 1273 K and then cooled at 1.8 K h^{-1} to 1173 K. To distinguish between these two phases, the monoclinic phase is hereafter referred to as α-$(Na_{3/4}K_{1/4})AlGeO_4$, while the hexagonal phase is referred to as β-$(Na_{3/4}K_{1/4})AlGeO_4$.

The chemical compositions of both $(Na_{3/4}K_{1/4})$-$AlGeO_4$ phases were determined by electron microprobe analysis, which was conducted by Dr C. Cermignani at the University of Toronto's Department of Geology. One crystal of each compound was analysed twice for its Na, K, Al and Ge content, and the results of the analyses are presented in Table 1. They clearly indicate that the hexagonal phase corresponds to a higher Na/K ratio than the monoclinic phase (4:1 *versus* 3:1, respectively). Furthermore, they reveal a slight alkali deficiency in the hexagonal phase, which is compensated by a higher Ge/Al ratio according to the substitution reaction: $A^+ + Al^{3+} = \square + Ge^{4+}$ (A = Na, K; □ = vacancy). Owing to the lack of suitable germanate standards to calibrate the microprobe (Cermignani, personal communication), the nominal composition of $(Na_{3/4}K_{1/4})AlGeO_4$ was assumed for the monoclinic phase, in good agreement with the structure solution (see below). This phase was then used as a calibration standard for the analysis of the hexagonal β-phase, yielding the composition $(Na_{0.78}K_{0.19})Al_{0.97}Ge_{1.03}O_4$.

Using crushed flux-grown crystals, powder X-ray diffraction patterns were recorded for both monoclinic and hexagonal $(Na_{3/4}K_{1/4})AlGeO_4$ using a Guinier–Hägg camera (Cu $K\alpha_1$ radiation) and were measured using a KEJ-LS20 digital scanner. The powder pattern for α-$(Na_{3/4}K_{1/4})AlGeO_4$ was indexed on the nepheline-like monoclinic cell: a = 10.0399 (8), b = 8.570 (1), c = 10.2045 (8) Å, β = 119.01 (1)°. This is the same cell as that reported by Barbier & Fleet (1988), although it is presented in an alternate setting with the b axis unique rather than the c axis. The observed powder pattern is given in Table 2, together with line intensities calculated using the program *XPOW* (Downs *et al.*, 1993) and the atomic positions determined from the single crystal data (see Table 9). The fit between the observed and calculated patterns is generally good, with some discrepancies in intensities due to the limitations of the scanner software for calculating integrated intensities of very closely spaced lines.

The powder pattern for β-$(Na_{3/4}K_{1/4})AlGeO_4$ was indexed on the nepheline-type hexagonal unit cell: a = 10.1795 (7), c = 8.5501 (1) Å. The observed pattern is presented in Table 3, together with one calculated using the program *XPOW* (Downs *et al.*, 1993) and the atomic positions obtained from the single crystal data (see Table 5). There is, in this case, a good fit between the observed and calculated intensities.

3. X-ray measurements and structure refinement

The X-ray intensity measurements for α-$(Na_{3/4}K_{1/4})$-$AlGeO_4$ were performed at the Siemens facility in Madison, Wisconsin, on a J413 diffractometer equipped with a CCD area detector using Mo $K\alpha$ radiation. The data for β-$(Na_{3/4}K_{1/4})AlGeO_4$ were measured at McMaster University on a Siemens *R3m/V* diffractometer system using Ag $K\alpha$ radiation. Both data sets were empirically corrected for absorption using the ψ-scan method.

The structure of α-$(Na_{3/4}K_{1/4})AlGeO_4$ was solved by direct methods in the space group $P2_1$ using data collected on a twinned crystal. All the crystals examined displayed a non-merohedral twinning which results from rotation about the pseudo-threefold axis of the pseudo-hexagonal unit cell (*i.e.* $\beta \simeq 120°$). The refinement of the anisotropic structure model against F^2 proceeded smoothly, using reflections corresponding to only one of the non-merohedral twin components of the crystal. During the refinement it was determined that further twinning was present corresponding to a chiral twin component within the non-merohedral twin component of the crystal over which the data was collected. Refinement of the chiral twin parameter indicated that the merohedral inversion (chiral) twin volume was 13 (2) vol% of the measured non-merohedral twin component of the crystal. The refinement was completed using a fully anisotropic model and gave a

Table 2. *Powder X-ray diffraction pattern of α-($Na_{3/4}K_{1/4}$)[$AlGeO_4$] from 10 to 40° in 2θ*

Observed intensities were measured using a KEJ LS-20 line scanner. Calculated intensities are reported where $I_{cal} > 1.0$ and are based on the single crystal data (*cf.* Table 8).

hkl	d_{cal} (Å)	d_{obs} (Å)	I_{cal}	I_{obs}
110	6.1326	6.1329	1.3	2.5
$\bar{1}11$	6.1121	—	1.1	—
101	5.1364	5.1407	1.9	3.4
$\bar{1}02$	5.1004	5.1018	1.9	2.8
002	4.4622	4.4619	13	16
111	4.4056	—	14	—
200	4.3902	4.3840	12	36
$\bar{1}12$	4.3828		19	
$\bar{2}02$	4.3603	4.3576	13	17
$\bar{2}11$	4.3313	4.3288	27	36
020	4.2845	4.2885	100	100
012	3.9577	3.9570	62	82
210	3.9073	3.9058	58	100
$\bar{2}12$	3.8861	3.8861	53	54
021	3.8625	—	2.3	—
120	3.8505	3.8470	2.0	10
$\bar{1}21$	3.8455		5.0	
102	3.3720	—	8.1	—
$\bar{1}03$	3.3550	3.3511	22	84
201	3.3484		31	
$\bar{2}03$	3.3218	3.3214	19	28
$\bar{3}01$	3.2940	—	1.2	—
302	3.2845	3.2846	9.8	17
112	3.1378	†	6.5	†
211	3.1187	3.1171	2.6	4.9
$\bar{2}13$	3.0972	—	8.0	—
022	3.0905	3.0906	41	76
$\bar{3}11$	3.0669	3.0651	4.8	94
220	3.0663		48	
$\bar{2}22$	3.0561	3.0561	42	63
003	2.9748	2.9744	23	34
300	2.9268	2.9268	22	40
$\bar{3}03$	2.9068	2.9069	31	52
122	2.6498	—	3.0	—
$\bar{1}23$	2.6415	2.6395	13	49
221	2.6383		15	
$\bar{2}23$	2.6252	2.6247	3.1	6.1
$\bar{3}21$	2.6114	—	1.2	—
$\bar{3}22$	2.6067	2.6066	17	30
202	2.5682	2.5679	15	20
$\bar{2}04$	2.5502	2.5499	10	15
$\bar{4}02$	2.5099	2.5095	3.4	3.3
131	2.4963	—	4.7	—
$\bar{1}32$	2.4922	2.4926	10	24
$\bar{2}31$	2.4826	—	5.4	—
103	2.4761	2.4762	12	12
212	2.4601	—	1.1	—
$\bar{2}14$	2.4443	2.4433	3.4	5
$\bar{3}04$	2.4317	—	4.7	—
$\bar{4}01$	2.4212	2.4214	16	28
320	2.4168	—	1.6	—
032	2.4057	2.4054	27	50
$\bar{3}23$	2.4055		2.6	
230	2.3942	2.3931	34	81.7
$\bar{2}32$	2.3893		40	
113	2.3788	—	1.8	—
$\bar{1}14$	2.3704	2.3699	9.6	15
311	2.3568	2.3575	4.5	6.1
$\bar{3}14$	2.3394	—	1.2	—
$\bar{4}11$	2.3300	2.3300	9.8	14
$\bar{4}13$	2.3210	2.3211	11	17

† Coincident with the Si standard line.

Table 3. *Powder X-ray diffraction pattern of ($Na_{0.78}K_{0.19}$)[$Al_{0.97}Ge_{1.03}O_4$] from 10 to 60° in 2θ*

Observed intensities were measured using a KEJ LS-20 line scanner. Calculated intensities are reported where $I_{cal} > 5.0$ and are based on the single crystal data (*cf.* Table 5).

hkl	d_{cal} (Å)	d_{obs} (Å)	I_{cal}	I_{obs}
200	4.407	4.399	25	33
111	4.3736	4.3731	34	25
002	4.2753	4.2717	61	60
201	3.9179	3.9137	100	100
120	3.3320	3.3311	11	55
210			36	
121	3.1046	3.1030	11	12
211			0.9	
202	3.0689	3.0677	70	71
300	2.9386	2.9385	45	37
122	2.6281	2.6281	5.2	21
212			26	
220	2.5449	2.5457	16	16
113	2.4868	2.4877	10	12
130	2.4450	2.4432	18	15
310			0.2	
203	2.3934	2.3929	57	56
131	2.3508	2.3515	6.3	19
311			15	
004	2.1376	2.1375	8.5	10
132	2.1224	2.1226	10	9.2
312			2.0	
231	1.9682	1.9681	10	7.4
321			3.7	
322	1.8282	—	8.3	—
501	1.7268	1.7284	10	8.7
233	1.6494	1.6500	14	18
323			5.0	
205	1.5943	1.5945	17	24

final $wR(F^2) = 0.12$ for all 4449 reflections [$R(F) = 0.055$ for all 2753 observed reflections]. Details of the crystal data, data collection and structure refinement are provided in Table 4.†

The β-($Na_{3/4}K_{1/4}$)$AlGeO_4$ structure was solved by direct methods in the hexagonal space group $P6_3$, initially assuming an ideal composition. The refinement of the isotropic model against F^2 proceeded smoothly, but gave a higher than expected value for $wR \simeq 0.25$. This, and large uncertainties on the atomic displacement parameters, suggested that the crystal might be twinned. Using a (110) mirror plane for the twin law improved the refinement, but also revealed that the crystal contained an inversion (chiral) twin. Refinement of the fractional volume of each twin component in the crystal resulted in values of 26 (3) vol% for the mirror twin, 26 (3) vol% for the chiral twin and 34 (3) vol% for a combined mirror and chiral twin, with the remainder (~14%) representing the untwinned component. All the atoms were allowed to refine anisotropically in the

† Lists of atomic coordinates, anisotropic displacement parameters and structure factors have been deposited with the IUCr (Reference: BR0065). Copies may be obtained through The Managing Editor, International Union of Crystallography, 5 Abbey Square, Chester CH1 2HU, England.

Table 4. *Experimental details*

	Hexagonal nepheline	Monoclinic nepheline
Crystal data		
Chemical formula	$Al_{0.97}Ge_{1.03}K_{0.19}Na_{0.78}O_4$	$AlGeK_{0.25}Na_{0.75}O_4$
Chemical formula weight	190.31	190.59
Cell setting	Hexagonal	Monoclinic
Space group	$P6_3$	$P2_1$
a (Å)	10.1640 (10)	10.0477 (4)
b (Å)		8.5764 (4)
c (Å)	8.540 (2)	10.2118 (4)
β (°)		119.0350 (10)
V (Å^3)	764.0 (2)	769.39 (6)
Z	8	8
D_x (Mg m^{-3})	3.294	3.291
Radiation type	Ag $K\alpha$	Mo $K\alpha$
Wavelength (Å)	0.56086	0.71073
No. of reflections for cell parameters	20	–
θ range (°)	5–30	–
μ (mm^{-1})	4.477	8.410
Temperature (K)	293 (2)	293 (2)
Crystal form	Hexagonal prism	Irregular prism
Crystal size (mm)	0.14 × 0.07 × 0.06	0.07 × 0.05 × 0.05
Crystal color	Colorless	Colorless
Data collection		
Diffractometer	Siemens *R3mV*	Siemens J413
Data collection method	θ–2θ scans	CCD area detector
Absorption correction	Empirical ψ scans *SHELXL*93 (Sheldrick, 1993)	Empirical from ψ scans *SHELXL*93 (Sheldrick, 1993
T_{min}	0.644	0.762
T_{max}	0.752	0.928
No. of measured reflections	6480	4438
No. of independent reflections	3060	3194
No. of observed reflections	1380	2753
Criterion for observed reflections	$I > 2\sigma(I)$	$I > 2\sigma(I)$
R_{int}	0.0853	0.0322
θ_{max} (°)	30.06	28.27
Range of h, k, l	$0 \rightarrow h \rightarrow 18$ $-18 \rightarrow k \rightarrow 0$ $-15 \rightarrow l \rightarrow 15$	$-13 \rightarrow h \rightarrow 13$ $-11 \rightarrow k \rightarrow 11$ $-13 \rightarrow l \rightarrow 8$
No. of standard reflections	3	–
Frequency of standard reflections	Every 100 reflections	–
Intensity decay (%)	None	–
Refinement		
Refinement on	F^2	F^2
$R[F^2 > 2\sigma(F^2)]$	0.0411	0.0554
$wR(F^2)$	0.0560	0.120
S	0.903	1.126
No. of reflections used in refinement	3060	3194
No. of parameters used	90	255
H-atom treatment	H-atom parameters not refined	H-atom parameters not refined
Weighting scheme	$w = 1/[\sigma^2(F_o^2) + (0.0109P)^2 + 0.0000P]$, where $P = (F_o^2 + 2F_c^2)/3$	$w = 1/[\sigma^2(F_o^2) + (0.0236P)^2 + 14.7287P]$, where $P = (F_o^2 + 2F_c^2)/3$
$(\Delta/\sigma)_{max}$	−0.001	0.001
$\Delta\rho_{max}$ (e Å^{-3})	1.010	1.679
$\Delta\rho_{min}$ (e Å^{-3})	−0.893	−1.142
Extinction method	*SHELXL*93 (Sheldrick, 1993)	*SHELXL*93 (Sheldrick, 1993)
Extinction coefficient	0.0028 (3)	0.0002 (4)
Source of atomic scattering factors	*International Tables for Crystallography* (1992, Vol. C)	*International Tables for Crystallography* (1992, Vol. C)
Computer programs		
Structure solution	*SHELXS*86 (Sheldrick, 1990)	*SHELXS*86 (Sheldrick, 1990)
Structure refinement	*SHELXL*93 (Sheldrick, 1993)	*SHELXL*93 (Sheldrick, 1993)

final model, with the exception of the O1 position, which was clearly non-positive definite when refined anisotropically. This result may be due to the large amount of twinning in this crystal and the fact that the O1 site is already split in the model (*i.e.* shifted from the threefold axis, *cf.* Table 5) in order to prevent the formation of an unfavourable 180° Al—O1—Ge bond angle (Liebau, 1985).

At this point, the equivalent isotropic displacement parameter (U_{eq}) of the K site was substantially higher than that observed for the Na site [0.0667 (11) *versus* 0.0287 (6) Å^2]. The results of the microprobe analysis indicated that the composition of the hexagonal crystal was not that of an ideal nepheline [*i.e.* $(Na_{3/4}K_{1/4})AlGeO_4$], but $(Na_{0.78}K_{0.19})Al_{0.97}Ge_{1.03}O_4$, with a small deficiency in K and a slight excess of Na as well as a slight excess of Ge (*cf.* Table 1). The occupancy of the K site was therefore adjusted to be 76% K, 12% Na and 12% vacant to reflect this change in composition, and a refinement of the new model was carried out. The results showed a significant improvement, with a decrease in U_{eq} for the mixed K/Na site from 0.0667 (11) to 0.0438 (9) Å^2, a decrease in $wR(F^2)$ from 0.091 to 0.071 and a decrease in the weighting parameter from 0.0252 to 0.0109. The model was further improved to account for the change in framework stoichiometry. Both the Al sites were assigned a composition of 97% Al and 3% Ge, based on the microprobe analysis. The final model gave $wR(F^2)$ = 0.066 for all 6480 reflections [$R(F)$ = 0.041 for 1380 observed reflections]. The details of the crystal data, data collection and refinement are given in Table 4.

4. Description of the hexagonal β-$(Na_{3/4}K_{1/4})AlGeO_4$ structure

The atomic coordinates and equivalent isotropic displacement parameters for β-$(Na_{3/4}K_{1/4})AlGeO_4$ are listed in Table 5. The U_{eq} values are larger for β-$(Na_{3/4}K_{1/4})AlGeO_4$ than those observed in the α-phase (*cf.* Table 8), reflecting the greater number of twin components in the refinement. This would result in a higher degree of disorder within the crystal structure, which the refinement compensates for by using higher displacement parameters. Bond lengths and selected bond angles for the β-$(Na_{3/4}K_{1/4})AlGeO_4$ structure are listed in Table 6.

Fig. 1 shows the β-$(Na_{3/4}K_{1/4})AlGeO_4$ structure viewed along the *c* axis. It is isostructural with the well studied mineral phase nepheline, $(Na_{3/4}K_{1/4})AlSiO_4$ (Hahn & Buerger, 1955; Dollase, 1970; Foreman & Peacor, 1970; Simmons & Peacor, 1972; Gregorkiewitz, 1984). When viewed down the *c* axis, the structure appears to contain a mirror plane at $z = 0, \frac{1}{2}$ (*cf.* Fig. 1), but, in fact, the mirror symmetry is broken by the Al/Ge ordering in the framework and also by the atomic coordinates [*i.e.* z = 0.1866 (6) for Al1, but z = 0.8000 (3) for Ge3; see Table 5]. Attempts to refine the structure in $P6_3/m$, which requires a disordered Al/Ge framework, were completely unsuccessful. The strong pseudo-mirror symmetry appears because of the similarity in the length of the Ge—O and Al—O bonds (~1.72 and 1.73 Å, respectively; see Table 6), while it is

Table 5. *Fractional atomic coordinates and equivalent isotropic displacement parameters (Å^2) for hexagonal nepheline*

$U_{eq} = (1/3)\Sigma_i\Sigma_j U^{ij}a^i a^j \mathbf{a}_i.\mathbf{a}_j$.

	x	y	z	U_{eq}
K1	0.0	0.0	0.9975 (9)	0.0436 (9)
Na1	0.0	0.0	0.9975 (9)	0.0436 (9)
Na2	0.9945 (3)	0.4380 (3)	0.9964 (4)	0.0300 (5)
Al1	1/3	2/3	0.1866 (5)	0.0115 (8)
Ge1	1/3	2/3	0.1866 (5)	0.0115 (8)
Al2	0.0897 (3)	0.3325 (5)	0.6810 (2)	0.0130 (3)
Ge2	0.0897 (3)	0.3325 (5)	0.6810 (2)	0.0130 (3)
Ge3	1/3	2/3	0.8000 (3)	0.0176 (3)
Ge4	0.08990 (9)	0.3336 (2)	0.30804 (9)	0.01645 (11)
O1†	0.2664 (12)	0.6124 (13)	0.9948 (21)	0.027 (3)
O2	0.0158 (5)	0.3147 (6)	0.4953 (6)	0.0434 (13)
O3	0.1643 (7)	0.5186 (7)	0.7401 (9)	0.056 (3)
O4	0.1639 (7)	0.5181 (6)	0.2510 (9)	0.052 (3)
O5	0.2232 (4)	0.2751 (5)	0.3141 (12)	0.0253 (13)
O6	0.2254 (6)	0.2762 (6)	0.6756 (7)	0.0239 (14)

† O1 site is 1/3 occupied. The O1 atom has been displaced from the 2(*b*) position at $(\frac{1}{3}\ \frac{2}{3}\ z)$ on the threefold axis and is split over the lower symmetry 6(*c*) position.

Table 6. *Bond lengths (Å) and selected angles (°) for β-$(Na_{3/4}K_{1/4})[AlGeO_4]$*

K1—O6^{i}	3.001 (7)	K1—O6^{ii}	3.001 (7)
K1—O6^{iii}	3.001 (7)	K1—O5^{iii}	3.012 (7)
K1—O5^{i}	3.012 (7)	K1—O5^{ii}	3.012 (7)
K1—O2^{i}	3.122 (5)	K1—O2^{ii}	3.122 (5)
K1—O2^{iii}	3.122 (5)	⟨K1—O⟩†	3.045
Na2—O1^{iv}	2.425 (11)	Na2—O6^{v}	2.496 (6)
Na2—O5^{v}	2.527 (8)	Na2—O2^{vi}	2.567 (5)
Na2—O4^{vii}	2.637 (9)	Na2—O3^{iv}	2.650 (8)
Na2—O3^{vi}	2.801 (8)	Na2—O4^{vi}	2.811 (8)
⟨Na2—O⟩	2.614		
Al1—O4^{viii}	1.717 (6)	Al1—O4	1.717 (6)
Al1—O4^{ix}	1.717 (6)	Al1—O1^{x}	1.75 (2)
⟨Al1—O⟩‡	1.726	Al2—O3	1.724 (7)
Al2—O2	1.725 (5)	Al2—O5^{ii}	1.732 (8)
Al2—O6	1.738 (5)	⟨Al2—O⟩‡	1.730
Ge3—O3^{viii}	1.701 (6)	Ge3—O3	1.701 (6)
Ge3—O3^{ix}	1.701 (6)	Ge3—O1	1.78 (2)
⟨Ge3—O⟩	1.720	Ge4—O4	1.706 (6)
Ge4—O6^{xi}	1.721 (6)	Ge4—O5	1.731 (4)
Ge4—O2	1.737 (5)	⟨Ge4—O⟩	1.724
Ge3—O1—Al1^{xii}	138.5 (6)	Ge4—O2—Al2	133.8 (2)
Ge3—O3—Al2	138.9 (4)	Ge4—O4—Al1	139.1 (4)
Ge4—O5—Al2^{xiii}	137.1 (6)	Ge4^{i}—O6—Al2	137.2 (4)

Symmetry codes: (i) $y, -x+y, z+\frac{1}{2}$; (ii) $x-y, x, z+\frac{1}{2}$; (iii) $-x, -y, z+\frac{1}{2}$; (iv) $x+1, y, z$; (v) $x-y+1, x, z+\frac{1}{2}$; (vi) $-x+1, -y+1, z+\frac{1}{2}$; (vii) $x+1, y, z+1$; (viii) $-x+y, -x+1, z$; (ix) $-y+1, x-y+1, z$; (x) $-x+y, -x+1, z-1$; (xi) $x-y, x, z-\frac{1}{2}$; (xii) $x, y, z+1$; (xiii) $y, -x+y, z-\frac{1}{2}$. † Actual site composition: 76% K, 12% Na and 12% vacant. ‡ Actual site composition: 97% Al and 3% Ge.

less pronounced in the natural nephelines owing to the greater difference in size between the Si—O and Al—O bond lengths (~1.64 and 1.77 Å; Shannon, 1976).

Two types of ring are observed in the β-$(Na_{3/4}K_{1/4})AlGeO_4$ framework. The tetrahedra in both rings alternately point up (*U*) and down (*D*), giving *UDUDUD* topology. The larger K1 site is located in the middle of the undistorted hexagonal ring and has a coordination number of 9. The mean K1—O distance, 3.045 Å, is similar to the 3.02 Å distance observed in $(Na_{3/4}K_{1/4})AlSiO_4$ by Dollase (1970). The smaller Na2 atom is eight-coordinate and lies in the highly distorted oval rings. This distortion is interpreted as an indication that the channels are too large for a Na atom and have collapsed to improve the bonding around it. The average Na2—O distance in this structure is 2.614 Å and is comparable to the Na—O distance of 2.62 Å observed by Dollase (1970) in $(Na_{3/4}K_{1/4})AlSiO_4$. To prevent the formation of an unfavourable 180° Al1—O1—Ge3 bond angle (Liebau, 1985), the O1 atom has been displaced slightly from the threefold axis, reducing the angle to 138.2 (6)° (*cf.* Fig. 1). This displacement also has the effect of shortening the Na2—O1 distance, making it the shortest of the Na—O bonds (see Table 6). Further justification for disordering the O1 position was also provided by the high isotropic displacement parameter which was observed when the atom was constrained to the threefold axis ($U_{iso} \simeq 0.16$ Å^2). This problem was resolved when the constraint was lifted and the oxygen was statistically disordered over three positions.

The atomic displacement parameters of the tetrahedral Al and Ge atoms and of the O5 and O6 atoms show no marked anisotropy, while the O2 position shows a large anisotropy in the large value of the U^{22} parameter [0.101 (4) Å^2]. A similar result was observed by Dollase (1970) in his refinement of the $(Na_{3/4}K_{1/4})AlSiO_4$ structure. Similarly, the strong anisotropy in the large U^{33} parameter of O3 and O4 [0.130 (9) and 0.126 (9) Å^2, respectively] was also observed by Dollase (1970). The O2, O3 and O4 atoms form the longest of the alkali–oxygen bonds (see Table 6) and the direction of the largest component of their anisotropy is towards the nearest alkali atom (*i.e.* Na2, *cf.* Fig. 2), which would suggest that it arises from an effort to improve the bonding environment around the Na2 site. The higher value of the isotropic displacement parameter (U_{eq}) for the K1/Na1 site compared with that of the Na2 site [0.0436 (9) *versus* 0.0300 (5) Å^2] indicates that the former is less strongly bonded and this is confirmed by the bond-valence results (Σs_{ij} = 0.77/0.32 and 0.95, respectively). The exceptionally low bond-valence sum for Na1 clearly indicates that this site is not a suitable bonding environment for Na. Simmons & Peacor (1972) noted that chemical analyses of natural nephelines were consistently Si-enriched relative to the idealized composition $(Na_{3/4}K_{1/4})AlSiO_4$, with a corresponding number of vacancies on the K site to preserve charge balance. According to Simmons & Peacor (1972), the total number of vacancies is approximately a

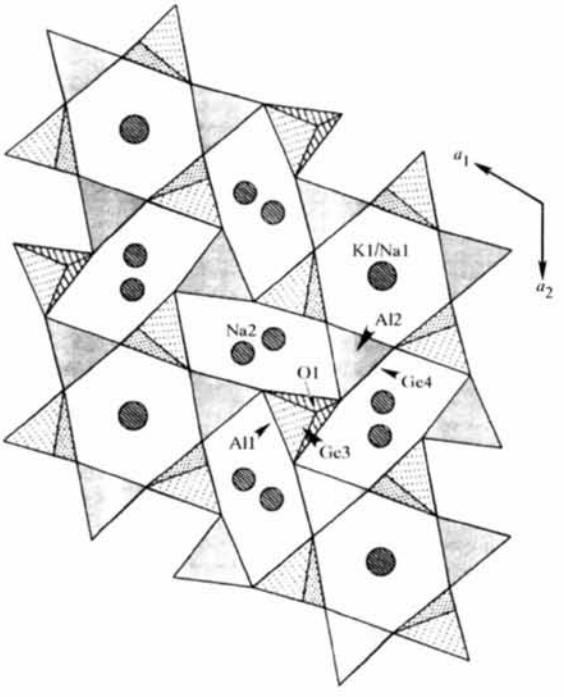

Fig. 1. The structure of β-$(Na_{3/4}K_{1/4})[AlGeO_4]$ viewed down the *c* axis of the hexagonal unit cell. The dotted shaded tetrahedra contain the Ge and Al atoms, respectively. The K and Na sites are shown as large and small circles, respectively. Note that the full unit cell, containing two layers of tetrahedra, is shown, but the lower half of the framework is eclipsed due to a pseudo-mirror plane perpendicular to the *c* axis. The complete ordering of the tetrahedral Al/Ge atoms precludes the existence of a true (001) mirror plane. Only one of the three partially occupied O1 positions is shown (*cf.* Table 5).

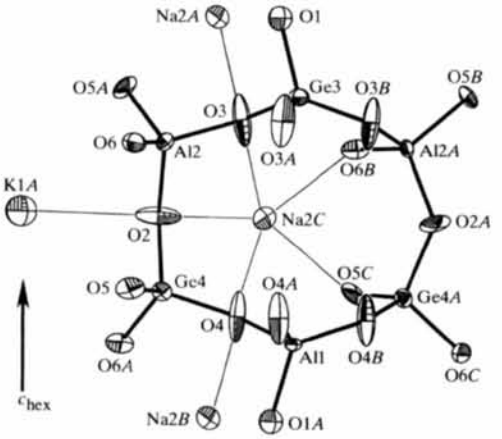

Fig. 2. An *ORTEP* (Johnson, 1965) plot of part of the β-$(Na_{3/4}K_{1/4})[AlGeO_4]$ structure viewed perpendicular to the *c* axis of the hexagonal unit cell.

Table 7. *Bond-valence ranges for cations and bond-valence sums for all atoms in β-($Na_{3/4}K_{1/4}$)[$AlGeO_4$], with bond-valence sums for ($Na_{3/4}K_{1/4}$)[$AlSiO_4$] (Foreman & Peacor, 1970) included for comparison*

All bond-valence data was calculated using the software package *STRUMOR* (Brown, 1989).

Atom	Bond-valence range	Valence sum (Σs_{ij}) β-($Na_{3/4}K_{1/4}$)-[$AlGeO_4$]	($Na_{3/4}K_{1/4}$)[$AlSiO_4$]
K1†	0.07–0.10	0.77	0.83
Na1†	0.03–0.04	0.32	–
Na2	0.06–0.19	0.95	0.92
Al1	0.70–0.77	3.01	3.11
Al2	0.73–0.75	2.97	2.93
*T*3‡	0.92–1.14	4.34	4.40
*T*4‡	1.03–1.12	4.27	4.28
O1		−1.82	−1.98
O2		−2.01	−2.05
O3		−2.06	−2.04
O4		−2.07	−1.95
O5		−2.06	−2.06
O6		−2.10	−2.05

† The site population of 76% K and 12% Na yields a weighted bond-valence sum of 0.62. ‡ *T* = Ge, Si where appropriate.

third of the available K sites. Similar results were reported for the refinement of a plutonic nepheline, $(Na_{0.68}K_{0.18}Ca_{0.04})[Al_{0.94}Si_{1.06}O_4]$, by Dollase (1970), who noted that the K1 site was only 61% occupied. This is considerably lower than the occupancy observed in β-($Na_{3/4}K_{1/4}$)$AlGeO_4$, for which this site has been determined as approximately 76% K, 12% Na and 12% vacant on the basis of the electron microprobe analysis.

Both the β-($Na_{3/4}K_{1/4}$)$AlGeO_4$ and ($Na_{3/4}K_{1/4}$)$AlSiO_4$ (Dollase, 1970) structures have similar valence sums (*cf.* Table 7). The K1 site is clearly underbonded in both structures with, in the germanate, a weighted bond-valence sum [76% Σs(K) + 12% Σs(Na)] equal to only 0.62. The distortion of the ring around the Na2 atom and the atom's shift from the centre of the ring (see Fig. 1) result in a much improved bonding arrangement for this atom (Σs_{ij} = 0.95). The bond-valence sums for the remaining atoms are within acceptable limits. In order to evaluate a structure based on the bond-valence sums around its component atoms, Salinas-Sanchez *et al.* (1992) have introduced the concept of a Global Instability Index (GII), which is defined as the root mean square of the bond-valence sum deviations for all of the atoms in the asymmetric unit

$$\mathrm{GII} = \left\{ \sum_{i=1}^{N} [(\sum_{j} s_{ij} - V_i)^2 / N] \right\}^{1/2},$$

where N represents the number of atoms in the asymmetric unit, s_{ij} is the bond-valence sum around atom j and V is the formal oxidation state of atom j. The value calculated for the GII of the β-phase is 0.17, similar to the value of 0.16 calculated for the ($Na_{3/4}K_{1/4}$)$AlSiO_4$ structure reported by Dollase (1970). Both these values are somewhat high and could indicate that there is strain imposed on the structure by the $P6_3$ symmetry.

Table 8. *Fractional atomic coordinates and equivalent isotropic displacement parameters (Å²) for monoclinic nepheline*

$U_{eq} = (1/3)\Sigma_i\Sigma_j U^{ij} a^i a^j \mathbf{a}_i.\mathbf{a}_j$.

	x	*y*	*z*	U_{eq}
Na1	0.4362 (5)	0.4289 (8)	0.4533 (5)	0.0201 (9)
Na2	0.5610 (5)	0.4288 (8)	0.9982 (5)	0.0222 (9)
Na3	0.0073 (5)	0.9293 (8)	0.4379 (5)	0.0228 (10)
K4	0.0121 (4)	0.4268 (6)	0.0077 (4)	0.0381 (7)
Ge1	0.34742 (13)	0.1227 (2)	0.66563 (12)	0.0099 (3)
Ge2	0.24343 (12)	0.6197 (2)	0.90195 (12)	0.0095 (2)
Ge3	0.08980 (12)	0.6157 (2)	0.34079 (12)	0.0097 (2)
Ge4	0.68052 (12)	0.6112 (2)	0.76134 (12)	0.0089 (2)
Al1	0.3474 (4)	0.7380 (5)	0.6649 (4)	0.0080 (7)
Al2	0.2448 (4)	0.2388 (5)	0.9032 (4)	0.0084 (7)
Al3	0.0901 (4)	0.2422 (5)	0.3414 (4)	0.0077 (7)
Al4	0.6810 (4)	0.2457 (5)	0.7631 (4)	0.0080 (7)
O1	0.4846 (10)	0.2334 (14)	0.6492 (11)	0.018 (2)
O2	0.7341 (8)	0.4307 (13)	0.7292 (8)	0.0127 (15)
O3	0.7384 (11)	0.2400 (13)	0.9531 (10)	0.017 (2)
O4	0.0527 (8)	0.6084 (16)	0.7721 (9)	0.016 (2)
O5	0.7772 (10)	0.1033 (16)	0.7209 (10)	0.017 (2)
O6	0.4863 (9)	0.6294 (18)	0.6473 (10)	0.019 (2)
O7	0.3587 (10)	0.1527 (11)	0.8405 (10)	0.018 (3)
O8	0.7337 (9)	0.6212 (18)	0.9506 (8)	0.017 (2)
O9	0.0511 (11)	0.2455 (13)	0.7715 (10)	0.016 (2)
O10	0.0177 (9)	0.4297 (13)	0.3332 (10)	0.022 (2)
O11	0.3040 (9)	0.4293 (13)	0.9611 (9)	0.023 (2)
O12	0.2252 (12)	0.2552 (12)	0.2799 (11)	0.013 (2)
O13	0.1656 (11)	0.6834 (12)	0.5210 (10)	0.020 (2)
O14	0.3900 (10)	−0.0675 (13)	0.6502 (10)	0.027 (2)
O15	0.1674 (11)	0.1700 (13)	0.5265 (12)	0.026 (3)
O16	0.3565 (11)	0.7026 (12)	0.8363 (11)	0.021 (2)

5. Description of the monoclinic α-($Na_{3/4}K_{1/4}$)$AlGeO_4$ structure

The final atomic coordinates and isotropic displacement parameters for α-($Na_{3/4}K_{1/4}$)$AlGeO_4$ are listed in Table 8. The uncertainties in the atomic positions are slightly larger than expected, particularly for the oxygen positions, likely as a result of the complex twinning in the crystal. Selected bond lengths and bond angles are given in Table 9.

Fig. 3 shows the α-($Na_{3/4}K_{1/4}$)$AlGeO_4$ structure viewed along the *b* axis. Note that the framework has a pseudo-mirror parallel to (010) so that the tetrahedra of the upper layer eclipse those in the lower layer. This pseudo-mirror plane is similar to that observed in the β-phase and, as in that case, the atomic coordinates (*cf.* Table 8) and the complete Al/Ge ordering prevent this from being a true mirror plane. The α-($Na_{3/4}K_{1/4}$)-$AlGeO_4$ structure is a slight monoclinic distortion of the hexagonal β-($Na_{3/4}K_{1/4}$)$AlGeO_4$ structure with the same nepheline-type *UDUDUD* topology, with two distinct ring types. Three-quarters of the rings have a highly

Table 9. *Bond lengths (Å) and selected bond angles (°) for α-($Na_{3/4}K_{1/4}$)[$AlGeO_4$]*

Na1—O14^{i}	2.441 (9)	Na1—O1	2.471 (12)
Na1—O6	2.483 (14)	Na1—O12	2.491 (12)
Na1—O5^{i}	2.509 (12)	Na1—O2	2.952 (9)
Na1—O6^{ii}	3.01 (2)	Na1—O1^{i}	3.058 (12)
⟨Na1—O⟩	2.676	Na2—O7^{iii}	2.400 (11)
Na2—O11	2.421 (9)	Na2—O16^{iv}	2.439 (12)
Na2—O8	2.606 (13)	Na2—O3	2.609 (12)
Na2—O7	3.025 (12)	Na2—O16	3.028 (12)
Na2—O14^{iii}	3.379 (12)	⟨Na2—O⟩	2.738
Na3—O4^{v}	2.462 (13)	Na3—O10^{v}	2.469 (9)
Na3—O9^{v}	2.486 (12)	Na3—O15^{vi}	2.501 (12)
Na3—O13	2.527 (12)	Na3—O13^{v}	2.942 (12)
Na3—O15^{v}	2.963 (12)	Na3—O14^{vi}	2.609 (12)
⟨Na3—O⟩	2.716		
K—O2^{vii}	2.860 (8)	K—O12	2.950 (10)
K—O5^{i}	2.959 (11)	K—O3^{vii}	2.993 (11)
K—O9^{viii}	3.051 (10)	K—O4^{viii}	3.055 (10)
K—O8^{vii}	3.059 (11)	K—O11^{viii}	3.191 (9)
K—O10	3.297 (9)	⟨K—O⟩	3.046
Ge1—O14	1.713 (12)	Ge1—O15	1.721 (10)
Ge1—O1	1.748 (10)	Ge1—O7	1.753 (9)
⟨Ge1—O⟩	1.734	Ge2—O4	1.724 (8)
Ge2—O16	1.728 (10)	Ge2—O3^{iii}	1.739 (10)
Ge2—O11	1.745 (11)	⟨Ge2—O⟩	1.734
Ge3—O13	1.715 (9)	Ge3—O9^{v}	1.727 (10)
Ge3—O5^{i}	1.735 (8)	Ge3—O10	1.739 (11)
⟨Ge3—O⟩	1.729	Ge4—O2	1.722 (11)
Ge4—O6	1.727 (9)	Ge4—O12^{i}	1.728 (10)
Ge4—O8	1.739 (7)	⟨Ge4—O⟩	1.727
Al1—O16	1.734 (10)	Al1—O14^{vi}	1.746 (12)
Al1—O6	1.758 (11)	Al1—O13	1.764 (10)
⟨Al1—O⟩	1.751	Al2—O7	1.726 (10)
Al2—O8^{iv}	1.727 (12)	Al2—O11	1.741 (11)
Al2—O9	1.749 (10)	⟨Al2—O⟩	1.736
Al3—O10	1.751 (12)	Al3—O12	1.754 (11)
Al3—O4^{xi}	1.762 (11)	Al3—O15	1.771 (11)
⟨Al3—O⟩	1.760	Al4—O3	1.736 (9)
Al4—O5	1.736 (12)	Al4—O1	1.741 (10)
Al4—O2	1.761 (11)	⟨Al4—O⟩	1.743
Ge1—O1—Al4	131.3 (6)	Ge4—O2—Al4	128.3 (4)
Ge2^{iv}—O3—Al4	144.0 (7)	Ge2—O4—Al3^{v}	135.7 (8)
Ge3^{ii}—O5—Al4	131.8 (8)	Ge4—O6—Al1	132.2 (7)
Ge1—O7—Al2	135.6 (6)	Ge4—O8—Al2^{iii}	146.3 (10)
Ge3^{xi}—O9—Al2	137.5 (7)	Ge3—O10—Al3	133.3 (5)
Ge2—O11—Al2	139.1 (5)	Ge4^{ii}—O12—Al3	130.7 (7)
Ge3—O13—Al1	136.5 (6)	Ge1—O14—Al1^{ix}	145.0 (5)
Ge1—O15—Al3	134.8 (6)	Ge2—O16—Al1	137.8 (6)

Symmetry codes: (i) $-x+1, y+\frac{1}{2}, -z+1$; (ii) $-x+1, y-\frac{1}{2}, -z+1$; (iii) $-x+1, y+\frac{1}{2}, -z+2$; (iv) $-x+1, y-\frac{1}{2}, -z+2$; (v) $-x, y+\frac{1}{2}, -z+1$; (vi) $x, y+1, z$; (vii) $x-1, y, z-1$; (viii) $x, y, z-1$; (ix) $x, y-1, z$; (x) $x, y, z+1$; (xi) $-x, y-\frac{1}{2}, -z+1$; (xii) $x+1, y, z+1$.

distorted oval shape and are occupied by the Na atoms with coordination number 8 and mean Na—O bond lengths 2.676 Å for Na1, 2.738 Å for Na2 and 2.716 Å for Na3. In order to achieve this coordination, the Na positions are also shifted significantly from the centre of the rings (*cf.* Fig. 3). The remaining quarter of the rings are undistorted and centred on the origin with the K atom sited near the centre of the ring. The K atom has the coordination number 9 and mean K—O bond length 3.046 Å. Note that the off-centre K position yields three short K—O bonds (*i.e.* K—O < 2.96 Å, *cf.* Table 9), while such short K—O distances are not found in the hexagonal β-phase structure (*cf.* Table 6).

As in the β-phase, the tetrahedrally coordinated Al and Ge atoms in the α-phase do not show any significant anisotropy in their atomic displacement parameters. As seen in Fig. 4, most of the O atoms are similarly well behaved and do not exhibit the strong anisotropy observed in the β-phase (*cf.* Fig. 2). A tendency towards non-positive definite values was only observed for the displacement parameters of the O1, O3, O10 and O11 atoms and this was probably an artefact of the refinement caused by the twinned nature of the crystal. It is noteworthy that the reduced anisotropy in the α-phase relative to the β-phase is accompanied by the formation of a larger number of shorter bonds around the Na atoms as well as around the K atoms (*cf.* Table 9).

The bond-valence sums for the α-($Na_{3/4}K_{1/4}$)$AlGeO_4$ structure are given in Table 10. They show a clear underbonding of the K position ($\Sigma s_{ij} = 0.80$), which is consistent with the higher U_{eq} observed for this site

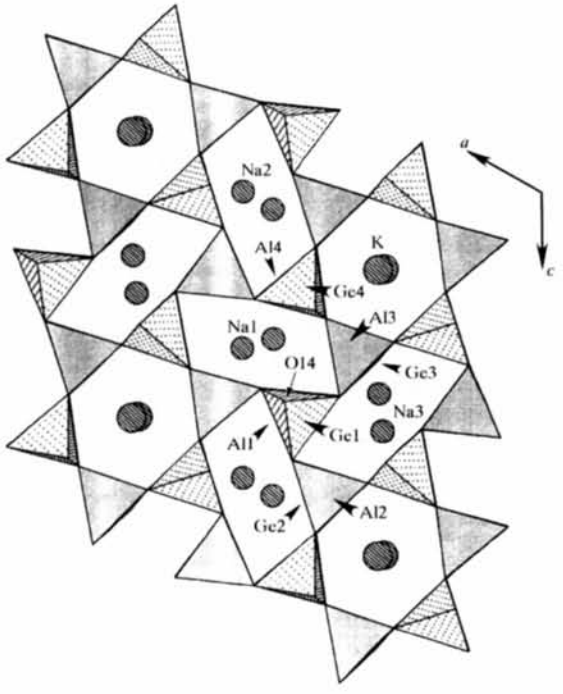

Fig. 3. The structure of α-($Na_{3/4}K_{1/4}$)[$AlGeO_4$] viewed down the *b* axis of the monoclinic unit cell. The dotted and shaded tetrahedra contain the Ge and Al atoms, respectively. The K and Na sites are shown as large and small circles, respectively. As in the structure of the hexagonal β-phase (*cf.* Fig. 1), the apparent (010) mirror symmetry is destroyed by complete Al/Ge ordering on the tetrahedral sites. Also note that, with the reduction to monoclinic symmetry, the K atom is no longer constrained to lie on the 6_3 axis and has shifted slightly (~0.1 Å) from the centre of the hexagonal rings. Also, the O14 position now corresponds to a fully occupied general position (*cf.* Table 8).

[U_{eq} = 0.0381 (7) Å^2; *cf.* Table 8]. However, as the site is fully occupied by K atoms in the monoclinic phase, the underbonding is not as severe as that observed for the corresponding K1/Na1 site in the hexagonal phase. The bond-valence sums also show a trend toward slight underbonding of the Na and Al atoms accompanied by a small overbonding of the Ge atoms, but the GII value of 0.11 for this structure is lower than that found for the β-phase (GII = 0.17), confirming that the decrease in symmetry has permitted an improvement in the overall bonding in the structure.

6. Discussion

The reduction from hexagonal to monoclinic symmetry between β- and α-$(Na_{3/4}K_{1/4})AlGeO_4$ corresponds to a decrease in space-group symmetry from $P6_3$ to $P2_1$, which eliminates the threefold axes in the unit cell. In the β-$(Na_{3/4}K_{1/4})AlGeO_4$ structure, these threefold axes constrain the K atom so that it sits on a (0,0,z) site at the centre of the undistorted hexagonal ring (*cf.* Fig. 1). However, with the lowering to monoclinic symmetry in the α-$(Na_{3/4}K_{1/4})AlGeO_4$ structure, the K atom occupies an (x,y,z) general position and shows a distinct shift of ~0.1 Å from the centre of the ring (*cf.* Fig. 3), resulting in some shorter and stronger K—O bonds (*cf.* Tables 6 and 9). The absence of threefold axes in the monoclinic structure also eliminates the need to disorder the oxygen positions, as found for the O1 atom in the hexagonal nepheline structures to prevent the formation of an energetically unfavourable 180° T—O1—T bond angle (Dollase, 1970; *cf.* Fig. 1 and Table 5). In α-$(Na_{3/4}K_{1/4})AlGeO_4$, the shift of the O14 atom from the pseudo-threefold axis (*cf.* Fig. 3 and Table 8) yields an Al1—O14—Ge1 bond angle of 145.0 (6)°, similar to the equivalent Al1—O1—Ge3 angle of 138.2 (6)° in β-$(Na_{3/4}K_{1/4})AlGeO_4$. Also, this shift yields a short Na1—O14 bond [2.441 (7) Å, *cf.* Table 9] in the α-phase comparable to the short Na2—O1 bond [2.425 (11) Å, *cf.* Table 6] in the β-phase. The lower monoclinic symmetry of the α-phase can also account for the reduced anisotropy of the atomic displacement parameters (*cf.* Figs. 2 and 4), the smaller values of the U_{eq} parameters (*cf.* Tables 5 and 8) and the improved bonding index (*cf.* previous section) by placing fewer constraints on the atomic positions, thus allowing the atomic positions to relax and to relieve any stresses in the bonding.

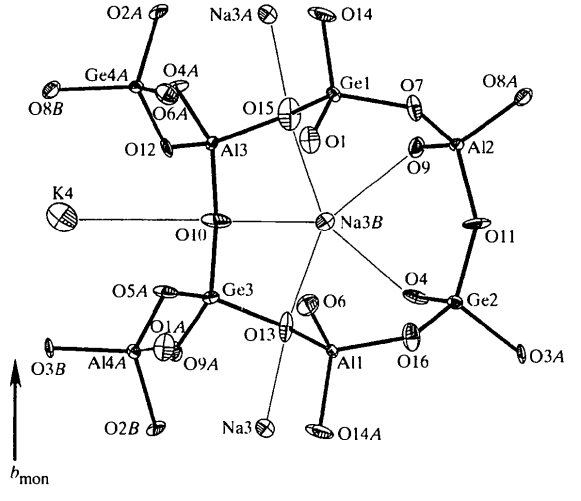

Fig. 4. An *ORTEP* (Johnson, 1965) plot of part of the α-$(Na_{3/4}K_{1/4})[AlGeO_4]$ structure viewed perpendicular to the b axis of the monoclinic unit cell.

Table 10. *Bond-valence ranges for cations and bond-valence sums for all atoms in* α-$(Na_{3/4}K_{1/4})[AlGeO_4]$, *calculated using the software package STRUMOR (Brown, 1989)*

Atom	Bond-valence ranges	Valence sum (Σs_{ij})
Na1	0.03–0.18	0.92
Na2	0.01–0.19	0.88
Na3	0.01–0.16	0.89
K	0.04–0.14	0.80
Al1	0.68–0.73	2.81
Al2	0.71–0.75	2.93
Al3	0.66–0.70	2.75
Al4	0.68–0.73	2.87
Ge1	0.99–1.10	4.16
Ge2	1.01–1.06	4.15
Ge3	1.02–1.09	4.21
Ge4	1.02–1.07	4.21
O1		−1.92
O2		−1.94
O3		−1.97
O4		−2.00
O5		−2.02
O6		−1.94
O7		−1.97
O8		−1.97
O9		−2.01
O10		−1.94
O11		−1.97
O12		−2.02
O13		−1.96
O14		−2.02
O15		−1.94
O16		−2.01

A comparison of the unit-cell volumes of the α- and β-phases reveals that the latter has a smaller cell [769.38 (9) *versus* 764.0 (2) Å^3, respectively]. The smaller volume of the β-phase is mainly due to a collapse along the hexagonal axis, as seen by comparing the equivalent unit-cell dimensions: $b(\alpha)$ = 8.5746 (4) *versus* $c(\beta)$ = 8.540 (2) Å, respectively. This difference is probably a consequence of the difference in the stoichiometry between the two phases: the K site is fully occupied in α-$(Na_{3/4}K_{1/4})AlGeO_4$, while in the β-phase this site contains 76% K, 12% Na and 12% vacancy, based on the microprobe analysis. The smaller size of the Na atom and the presence of vacancies in this site likely leads to a shrinking of the framework, resulting in

the decrease observed for the c axis in the β-phase. The $T-O-T$ interlayer bond angles in the β-phase [$T-O1-T$ = 138.2 (6) and $T-O2-T$ = 133.8 (6)°] also indicate that its tetrahedral framework is more collapsed than that of the α-phase [with corresponding values of 145.0 (6)° for the $T-O14-T$ angle and 133.6° for the average of the $T-O2-T$, $T-O10-T$ and $T-O11-T$ angles].

Although the hexagonal β-phase has a higher symmetry than the monoclinic α-phase, as expected for the high-temperature polymorph of a phase transition, the accompanying decrease in unit-cell volume is not typical. Coupled with the slight composition difference between the α- and β-phases and the absence of any thermal event in the DTA trace during heating and cooling cycles, these observations lead to the conclusion that the $\alpha \rightarrow \beta$ transition in $(Na_{3/4}K_{1/4})AlGeO_4$ is not truly polymorphic. The previous synthesis of a hexagonal phase from a $(Na_{3/4}K_{1/4})AlGeO_4$ melt slowly cooled between 1473 and 1273 K (Strunz & Ritter, 1961) may have also resulted from a composition change, possibly due to incongruent melting or loss of alkali oxide from the melt (note that no chemical analysis or structure determination was carried out in that earlier study). In the present study, the crystallization of the alkali-deficient hexagonal $(Na_{0.78}K_{0.19})Al_{0.97}Ge_{1.03}O_4$ phase from a flux enriched in MoO_3 may have been the result of a higher solubility of K_2O in that flux.

The authors wish to acknowledge the assistance of the following: Dr J. Britten of McMaster University and Dr C. Campana of Siemens Inc. for X-ray data collection, Dr C. Cermignani of the University of Toronto for the electron microprobe analyses, Mr F. Gibbs of McMaster University for the DTA measurements, and the Canadian Natural Sciences and Engineering Research Council for financial support.

References

Barbier, J. & Fleet, M. E. (1988). *Phys. Chem. Miner.* **16**, 176–285.

Brown, I. D. (1989). *J. Chem. Inf. Comput. Sci.* **29**, 266–271.

Dollase, W. A. (1970). *Z. Kristallogr.* **132**, 27–44.

Downs, R., Bartelmehs, K., Gibbs, G. & Boison Jr, M. (1993). *Am. Mineral.* **78**, 1104–1107.

Foreman, N. & Peacor, D. R. (1970). *Z. Kristallogr.* **132**, 45–70.

Gregorkiewitz, M. (1984). *Bull. Mineral.* **107**, 499–507.

Hahn, J. & Buerger, M. J. (1955). *Z. Kristallogr.* **106**, 308–388.

Johnson, C. K. (1965). Report ORNL-3794. Oak Ridge National Laboratory, Tennessee, USA.

Liebau, F. (1985). *Structural Chemistry of Silicates*, p. 260. New York: Springer-Verlag.

Salinas-Sanchez, A., Garcia-Muñoz, J. L., Rodríguez-Carvajal, J., Saez-Puche, R. & Martínez, J. L. (1992). *J. Solid State Chem.* **100**, 201–211.

Shannon, R. D. (1976). *Acta Cryst.* A**32**, 751–767.

Sheldrick, G. M. (1990). *SHELXTL/PC User's Manual.* Siemens Analytical X-ray Instruments Inc., Madison, Wisconsin, USA.

Sheldrick, G. M. (1993). *SHELXL93. Program for the Refinement of Crystal Structures.* University of Göttingen, Germany.

Simmons, W. B. & Peacor, D. R. (1972). *Am. Mineral.* **57**, 1711–1719.

Strunz, H. & Ritter, E. (1961). *Neues Jahrb. Miner. Monatsh.* **1**, 22–23.